ELSEVIER

Materials Science and Engineering A355 (2003) 338–347

MATERIALS SCIENCE & ENGINEERING A

www.elsevier.com/locate/msea

Development of hybrid materials consisting of SiO_2 microparticles embedded in phenolic-formaldehydic resin polymer matrices

G. Hernández-Padrón [a,*], F. Rojas [b], M. García-Garduño [c], M.A. Canseco [d], V.M. Castaño [a]

[a] *Centro de Física Aplicada y Tecnología Avanzada, UNAM, A.P. 1-1010, Querétaro, Querétaro 76000, Mexico*
[b] *Departamento de Química, Universidad Autónoma Metropolitana-Iztapalapa, Mexico, D.F., 09340, Mexico*
[c] *División de Estudios de Posgrado e Investigación, Facultad de Odontología, UNAM, México D.F., Circuito Institutos S/N, Cd. Universitaria, Mexico, D.F., 04510, Mexico*
[d] *Instituto de Materiales, UNAM, Circuito Interior S/N, Cd. Universitaria, Mexico, D.F., 04510, Mexico*

Received 4 June 2002; received in revised form 27 January 2003

Abstract

A phenolic-formaldehydic resin (PFR) of the Novolac-type and modified by the incorporation of carboxylic end groups (MPFR), is used to influence the morphological and optical properties of sol-gel synthesized SiO_2 materials. Silica microparticles are formed from the hydrolysis of silicon alkoxide solutions in ethanol and in the presence of polymerizing PFR or MPFR resins, hence rendering a final product consisting of SiO_2 globules entangled inside a resin network. Under appropriate experimental conditions, chemical unions are established between silanol groups anchored on the surface of the SiO_2 particles and MPFR carboxylic chains, to provide SiO_2/MPFR core-shell compounds. The presence of PFR or MPFR resins during the SiO_2 sol-gel production influences: (i) the size of SiO_2 particles; and (ii) the transparency, translucency or opacity properties of the final hybrid products. Either one of the latter optical conditions is established by the amounts of reactants used to prepare a given hybrid specimen. FTIR, TGA and SEM are employed to determine the chemical and textural properties of SiO_2/PFR and SiO_2/MPFR solids. Results confirmed the existence of chemical bonds at the interface between silica and MPFR resin, as well as superior properties of these hybrid materials with respect to pure PFR or MPFR polymerized materials.

Keywords: Hybrid silica materials; Hybrid phenolic-formaldehydic resin materials; Silica microspheres; Translucent silica materials; Opaque silica materials

1. Introduction

The quality of modern-day composites should be evaluated in terms of their optical, mechanical, electrical and biological characteristics [1]. Under this perspective, the features displayed by a composite material not only depend on the characteristics of the individual components, but also on the phase morphology and interfacial properties of the final hybrid product [2]. These latter features are paramount to foreseeing the overall quality of the final mixed material. More recently, the idea of producing synergetic single-phase materials (in which actual chemical bonds can be established across an interface thus making it very difficult to know where a given phase ends and the next one begins) has led to a whole new area of hybrid materials, i.e. products which are neither organic nor inorganic, but both at the same time.

In this work, with the purpose of producing novel hybrid organic–inorganic materials endowed of interesting optical, mechanical or thermal features, the general sol-gel reaction has been customized in order to create solids consisting of silica particles trapped inside a phenolic-aldehydic polymeric network [3,4]. Firstly, carboxylic end groups are chemically joined to the molecules of a Novolac-phenolic-formaldehydic

* Corresponding author. Tel.: +52-55-5623-4132; fax: +52-442-2381-165.
E-mail address: genoveva@servidor.unam.mx (G. Hernández-Padrón).

0921-5093/03/$ - see front matter
doi:10.1016/S0921-5093(03)00101-1

(PFR) resin in order to produce functionalized (i.e. modified) MPFR substrates. The –COOH functional groups that are attached to the MPFR molecules can then fully or partially react with compatible groups (e.g. silanol –Si–OH) anchored on the surfaces of the colloidal particles that are being formed during the hydrolysis-condensation of a silicon alkoxide. Therefore, chemical bonds established across the SiO_2–MPFR interface can cause the irreversible incorporation of the organic polymer molecules of interest onto the surfaces of the inorganic (silica) sol-gel particles. After pursuing a thermal treatment of this SiO_2–MPFR precursory hybrid system, a resin polymer network entrapping a collection of SiO_2 particles can be finally created. It is also pertinent to mention that by means of similar preparation methods, whole new families of hybrid materials have been previously synthesized, thus creating innovative mixed systems displaying a combination of the features of inorganic sol-gel alkoxide moieties with those of a variety of organic or inorganic species [5,6].

Here, it will be shown how a chemical adhesion of functionalized phenolic-formaldehydic resin molecules around the surface of colloidal silica particles does indeed result in a material showing interesting new properties. Analysis of this type of hybrid materials by FT-IR spectroscopy confirms the existence of additional chemical bonds, thus indicating a chemical interaction between groups on the surface of the SiO_2 particles and the functional groups of the MPFR molecules. These chemical bonds are mainly a consequence of the reaction between –Si–OH groups of the silica particles and the carboxylic end groups of the modified resin. TGA and SEM studies have also been employed to characterize the hybrid substrates with respect to their thermal and morphological properties.

2. Experimental

2.1. Materials

All hybrid samples were prepared by using tetraethylorthorsilicate (TEOS, 98% Aldrich), CO_2-free triple distilled water, ethanol, unmodified (PFR) or functionalized (MPFR) phenolic-formaldehydic Novolac type resins (materials that were synthesized and, if required, chemically modified in our laboratory in order to incorporate carboxylic end groups into the original phenolic-aldehydic resin molecules). Oxalic acid (J.T. Baker) and abietic acid (Aldrich) were the key reactants used for functionalizing the original Novolac resin with carboxylic end groups. HF, HCl or NH_4OH were employed as inorganic catalysts (IC) to accelerate the gelation process of either SiO_2/PFR or SiO_2/MFPR hybrid systems. In order to simplify sample identification, NH_4OH will be hereafter just labeled as NH_3.

2.2. Preparation of hybrid materials

The PFR resin (precursor of the MPFR) was synthesized through a conventional route for the Novolac-type [7] and successively functionalized with carboxylic end groups in order to create the MPFR resin. The methods of synthesis of PFR and MPFR resins have been fully described elsewhere [8] and in this work, the procedure to prepare the MPFR compound will be succinctly described in the following manner. First, the PFR Novolac-type resin was prepared through the careful mixing of 440 g (20.3 mol) of formaldehyde (F) and 685 g (25.6 mol) of phenol (P) (i.e. an F/P molar ratio of 0.79 was employed). This F–P mixing was followed by the dropwise addition of a solution containing 4.5 g of oxalic acid in 50 cm^3 of water. The resultant mixture was then left under refluxing conditions for 30 min. Immediately afterwards, a solution containing 4.5 g of abietic acid in 50 cm^3 of water was poured into the glass reactor and the reacting system was kept refluxing for a further 1 h. The reaction scheme illustrating the functionalization reaction occurring between PFR and abietic acid molecules is shown in Scheme 1.

The desired hybrid materials, constituted by silica (x% weight) and either PFR or MPFR resin (y% weight, $x+y=100$), were synthesized in an ethanol solution. Initially, a mixture of PFR or MPFR (4 g) and ethanol (20 cm^3) was prepared, while a second mixture involving TEOS (1.25–3.75 cm^3, the exact quantity depending on the desired final molar composition of the SiO_2–PFR or SiO_2–MPFR hybrid) in water (2 cm^3) together with ethanol (20 cm^3) was made separately. The two solutions were then poured simultaneously into a glass reactor and the resulting mixture was subjected to vigorous stirring and kept under refluxing conditions for 5 h. Diverse TEOS: H_2O molar ratios corresponding

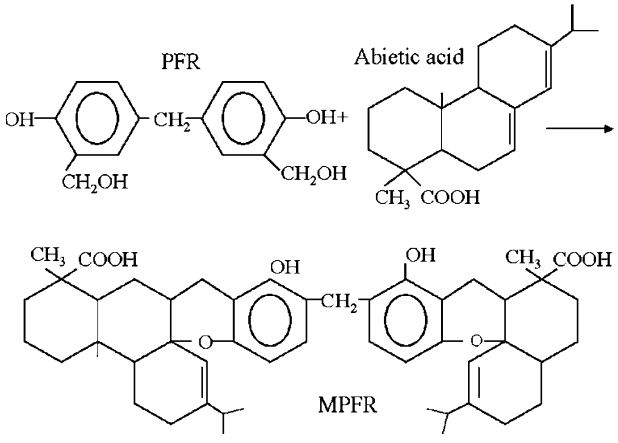

Scheme 1. Reaction scheme for the synthesis of MPFR.

to: (i) 1:8; (ii) 1:4; (iii) 3:8; (iv) 1:2; (v) 1.1:2; (vi) 5:8; and (vii) 3:4 were employed together with the 4 g of PFR or MPFR resin dissolved in 20 cm^3 of ethanol in order to obtain an assortment of hybrid compounds.

In every case, a sol could be distinguished at the end of the reaction time and the ensuing colloidal dispersion was stored in a glass flask for a long time (≈ 2 months) until gelation occurred; nevertheless, if desired, the time length of this process could be accelerated a great deal by the addition of a tiny amount (≈ 1 mm^3) of an inorganic catalyst, such as HF, HCl or NH_4OH (abbreviated NH_3). The gels were kept at room temperature and, depending (among other things) on the addition or not of an inorganic gelation catalyst, an *opaque* (i.e. a non-transparent specimen endowed with a dull coloration) or a *transparent-translucent* substrate (either having a slight amber or red coloration) was attained, respectively.

2.3. Characterization techniques

The characterization of the chemical groups existing in the hybrid materials was carried out by FTIR spectroscopy. This analysis was performed via a Nicolet 510 spectrometer, equipped with an Ar laser while applying the diffuse reflectance technique to powders made of mixtures of the hybrid material and KBr (1:2 weight ratio).

Scanning electron microscopy (SEM) observations were performed by means of a JEOL JSM-5200 microscope.

In turn, TGA analyses were carried out with a DuPont 951 instrument operated in air at a rate of 10 K min^{-1}.

3. Results and discussion

A large variety of hybrid materials were analyzed in this work. The following nomenclature is employed to facilitate the identification of a given compound among the diversity of specimens: (i) $SiO_2(x)$/PFR(y)/IC or (ii) $SiO_2(x)$/MPFR(y)/IC, where x and y $(x+y=100)$ represent the percent weight of each phase in the corresponding hybrid product. Several aspects of this nomenclature require further clarification: (i) when $x=0$, we have either pure PFR or MPFR polymer resins; and (ii) the addition of an inorganic acid or basic compound (denoted as IC after the idea that these substances constitute inorganic catalysts to speed up the sol→gel transition) during the synthesis of hybrid materials is denoted by HF, HCl or NH_3, otherwise none of these latter symbols would appear.

3.1. FTIR spectroscopy

FTIR spectra related to: (a) MPFR(100), (b) SiO_2(100) and (c) SiO_2(57)/MPFR(43) materials, are shown in Fig. 1. The MPFR(100) FT-IR spectrum confirms the functionalization of the original Novolac resin with carboxylic groups because of the presence of bands at 1698 cm^{-1} (C = O) and 1226 cm^{-1}; this latter signal attributed to the C–O–C ester group vibration, whose identification via FT-IR spectroscopy has been previously reported [8].

The spectrum of pure silica, SiO_2(100) shows a band at 1633 cm^{-1} owing to the O–CH_2 group [9] of ethanol (as this solvent is present throughout the sol-gel silica synthesis). Additionally, bands corresponding to Si–O–Si symmetric and asymmetric vibrations are located at 796 and 1104 cm^{-1}, respectively [10]. The signal at 959 cm^{-1} can be assigned to the Si–OH group [11], while the wider one, positioned in the range 3000–3800 cm^{-1}, is attributed to the presence of hydroxyl groups [12]. Finally, peaks at 2965 and 2907 cm^{-1} are due to ethanol organic groups [13].

The SiO_2(57)/MPFR(43) FTIR spectrum shows a band in the region between 2900 and 3000 cm^{-1}, a signal that is related to phenolic OH groups. CH stretching of phenyl rings is found in the 3000–3100 cm^{-1} region [14]. The ester carbonyl groups observed at 1690 cm^{-1} are evidence of the reaction between OH

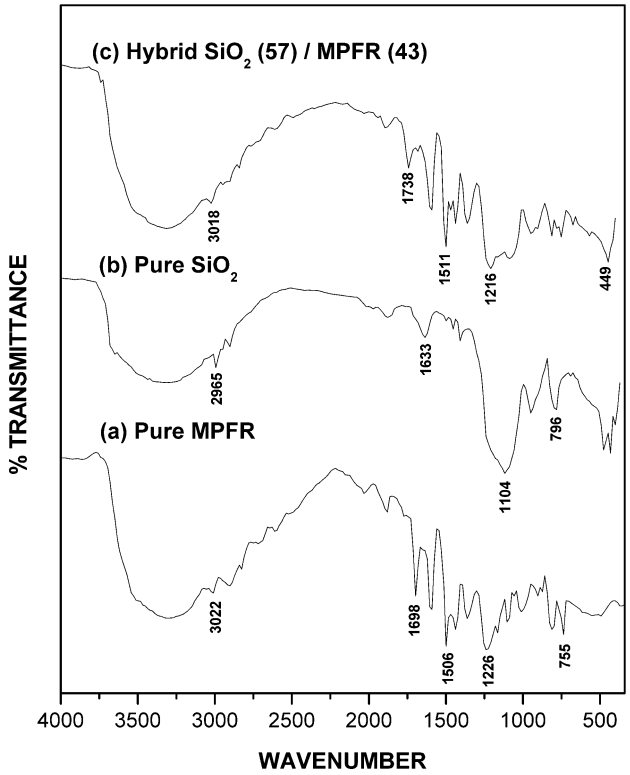

Fig. 1. FT-IR spectra of (a) MFPR (100), (b) silica (100) and (c) SiO_2(57)-MPFR(43) materials.

groups (belonging to carboxylic groups of the MPFR) and silanol groups on the surface of the silica particles [15]. This reaction is favored by the high electronegativity of oxygen and the readily available lone pair of electrons of the carbonyl group and also by the acidic nature of Si–OH groups. In this way, polymer chains of MPFR are chemically bonded to silanol groups on the surface of SiO_2 microspheres. It is also possible to observe that the band in the range 1200–900 cm^{-1} becomes wider (with respect to a similar signal that is provided by the spectrum of pure MPFR) because of the interaction between free OH groups of the resin and OH groups of the silica particles. A somewhat less evident widening effect occurs in the range 3700–3000 cm^{-1} due to the incorporation of silica inside the resin matrix; the width of this signal increases with the amount of TEOS involved during the synthesis of this hybrid material.

3.2. TGA measurements

TGA analyses can provide a picture of the thermal stabilities of SiO_2–MPFR hybrid materials with respect to pure PFR or MPFR polymerized resin specimens. Fig. 2 includes a comparative series of TGA spectra related to SiO_2(100), PFR(100), MPFR(100) and SiO_2(57)/MPFR(43) materials. In this figure, it can be seen that the thermal stability approximately decreases according to the following sequence: (i) SiO_2(100) > (ii) SiO_2 (57)/MPFR(43) > (iii) MPFR(100) > (iv) PFR(100). This succession thus gives some idea about the rather larger thermal stability of MPFR with respect to PFR and also of the increased stability caused by the presence of SiO_2 in the hybrid materials. For instance, at 1000 °C TGA residual masses are as follows: (i) SiO_2(100) 88 wt.%; (ii) SiO_2 (57)/MPFR(43) 46 wt.%; (iii) MPFR(100) 33 wt.%; and (iv) PFR(100) 20 wt.%.

Fig. 3 shows a series of TGA thermographs related to several $SiO_2(x)$/MPFR(y)/HF hybrid compounds of

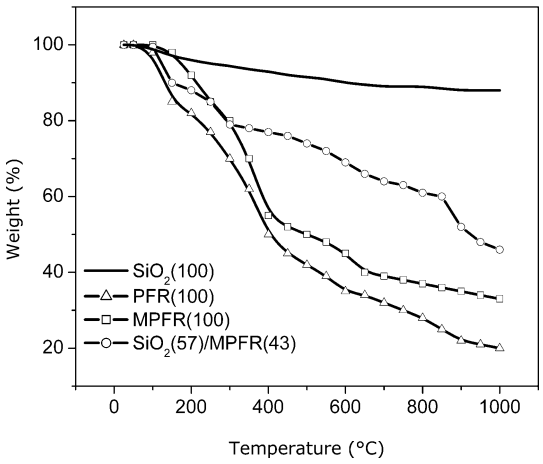

Fig. 2. TGA spectra of SiO_2(100), PFR(100), MPFR(100) and SiO_2(57)/MPFR(43) materials.

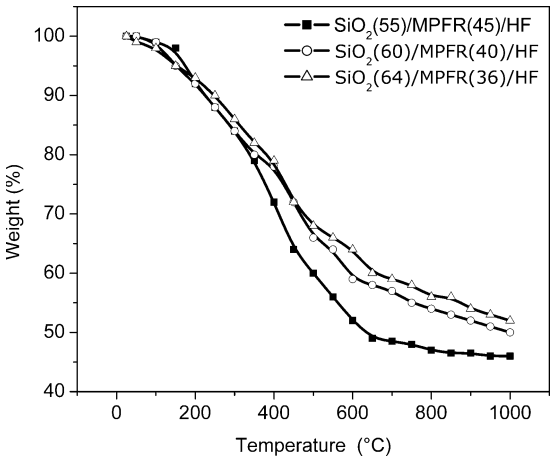

Fig. 3. TGA spectra of SiO_2(55)/MPFR(45)/HF, SiO_2(60)/MPFR(40)/HF and SiO_2(64)/MPFR(36)/HF hybrid materials.

different compositions. It is evident from this plot that the mounting presence of silica improves the thermal stability of a hybrid material. The weight-loss curves for these hybrid compounds show a kind of two-step degradation mechanism (see Fig. 3); there exists first a continual weight loss from low temperatures up to ≈ 570–650 °C, a behavior that is followed by a less intense decomposition pace that continues up to 1000 °C. On comparing the shapes of these thermal spectra with the TGA thermograph of pure MPFR (see Fig. 2), it can be seen that the presence of SiO_2 decreases the overall rate of degradation (in the range between room temperature and 1000 °C) of SiO_2–MPFR hybrid materials in comparison to the pure MPFR material. The TGA spectra of samples SiO_2(55)/MPFR(45)/HF and SiO_2(60)/MPFR(40)/HF show an intersection point occurring at ≈450 °C; this crossing is located around the transition region between the two thermal decomposition patterns [16]. Additionally, the thermographs of SiO_2(55)/MPFR(45)/HF, SiO_2(60)/MPFR(40)/HF and SiO_2(64)/MPFR(36)/HF materials depict an almost complete disappearance of MPFR, given that percent weight losses of 42, 40 and 35 (quantities that are closely related to the stoichiometric MPFR composition of these hybrid substrata) are observed just when the second decomposition stage is on the verge of starting, respectively. Consequently, it is pertinent to mention that this second decomposition stage occurs at temperatures around 620 °C (SiO_2(55)/MPFR(45)/HF), 650 °C (SiO_2(60)/MPFR(40)/HF) and 570 °C (SiO_2(64)/MPFR(36)/HF), correspondingly, for the set of hybrid compounds included in Fig. 3.

A comparison between the derivatives of the TGA thermographs of MPFR(100) and SiO_2(64)/MPFR(36) materials is shown in Fig. 4. The differential TGA curve of MPFR(100) involves a main peak at a temperature of ≈360 °C, while the hybrid material shows an intense decomposition between 400 and 540 °C, i.e. a positive

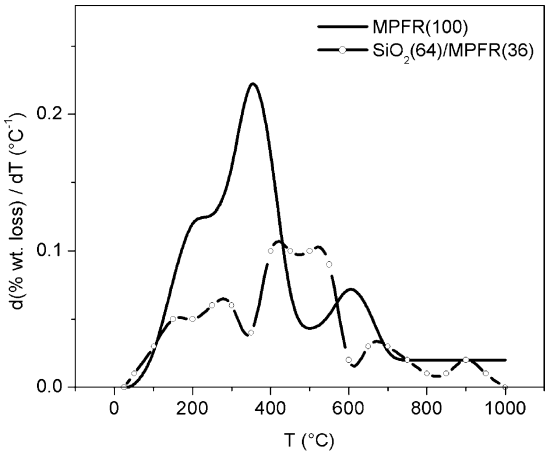

Fig. 4. Differential TGA spectra of MPFR(100) and SiO_2(64)/MPFR(36) materials.

displacement of 40–180 °C with respect to the silica-free MPFR substrate.

3.3. SEM characterization of hybrid materials

A SEM photographic study of SiO_2/MPFR and SiO_2/PFR materials was performed too. Table 1 (SiO_2/PFR) and Table 2 (SiO_2/MPFR) provide lists of the materials characterized by SEM together with some important observations about the morphologies as well as with respect to some other optical or interesting properties of these solids.

SEM micrographs of $SiO_2(x)$/PFR(y)/IC substrata are shown in Figs. 5–10. Here, it is possible to observe the diverse morphologies of these materials. Usually SiO_2 particle-size distributions inside the hybrid media are not too wide and consist of quasi-spherical micron-size silica particles embedded in the polymeric PFR medium.

In general, for these $SiO_2(x)$/PFR(y) systems, we can observe that the molar SiO_2/PFR ratio as well as the choice HF or HCL catalysts [6] determine their optical (transparency or opacity) properties. At high SiO_2 contents, the resulting materials are mostly opaque, especially if HF or NH_3 have been employed during the synthesis. In general, it seems that the lack of strong chemical interaction across the interface of silica particles and PFR resin contributes in some way to the opacity displayed by many of these substrata.

The microstructures of $SiO_2(x)$/MPFR(y) materials exhibit very interesting optical and morphological features (see Figs. 11–22). Generally speaking, the aggregation extent of silica particles (in the form of clusters that are distributed throughout the hybrid system) changes according to the specific experimental conditions (i.e. TEOS: H_2O molar ratio, type of catalyst, etc.) employed in the synthesis of $SiO_2(x)$/MPFR(y) solids; these SiO_2 cluster characteristics can induce phase separation [17], thus influencing a great deal the optical properties of the system [18]. Briefly speaking, both the SiO_2 mean particle size and the interfacial properties between silica and MPFR matrices allow obtaining either transparent or opaque materials depending on the preparation conditions. When the silica content is not too large, the hybrid materials are transparent-translucent specimens, independently of the catalyst used to promote gelation.

The crystals observed in sample SiO_2(40)/MPFR(60)/NH_3 (see Figs. 12 and 13) are part of a flake-like arrangement and the presence of NH_3 during the synthesis may be related to this crystalline formation (Fig. 14). At this point, it is pertinent to mention that some cubic crystals were observed in the SiO_2(55)/PFR(45)/HF system (see Figs. 6–8), although this time the material is opaque rather than a translucent material.

It seems that a hybrid SiO_2–MPFR material is rendered transparent when there is a homogeneous distribution of micrometric silica aggregates throughout the volume of the substrate, whereas it can become

Table 1
Characteristics of PFR substrata as observed by SEM

Material ID	Figure No.	Features
PFR(100)	Fig. 5	Transparent-amber. Smooth surface with some fractures. Trapped air bubbles.
SiO_2(47)/PFR(53)		Opaque-red. Evidence of coalesced, polydisperse SiO_2 particles embedded in PFR matrix.
SiO_2(47)PFR(53)/NH_3		Opaque-brown. Coalesced SiO_2 particles segregate from PFR matrix.
SiO_2(55)/PFR(45/HF	Figs. 6–8	Opaque-orange. SiO_2 crystals of ≈ 3 μm segregate on the outer surface of sample (Figs. 6 and 7). Fracture surfaces show coalesced SiO_2 particles embedded in the resin matrix (Fig. 8).
SiO_2(55)/PFR(45)/HCl		Transparent red. Very smooth surface with some cracks.
SiO_2(57)/PFR(43)	Figs. 9 and 10	Translucent-orange. Phase separation between silica and PFR matrix. Amorphous silica globules appear on outer surfaces.
SiO_2(57)/PFR(43)/HF		Opaque-orange. A fused mass of SiO_2 particles surrounded by PFR polymer.
SiO_2(57)PFR(43)/NH_3		Opaque-orange. Coalesced silica particles together with PFR polymer forming a flake-like structure.

Table 2
Characteristics of MPFR substrata as observed by SEM

Material ID	Figure No.	Texture features
MPFR(100)	Fig. 11	Transparent-amber. Sample is much more resistant than PFR(100).
SiO_2(40)/MPFR(60)/NH_3	Figs. 12–14	Translucent-red. Crystalline SiO_2 particles resting on a bed of silica particles (2.5 μm) and MPFR polymer (Figs. 12 and 14). Fracture surfaces include collections of flake-like crystals (Fig. 13).
SiO_2(47)/MPFR(53)/HF		Translucent-red. Threads of MPFR polymer surround SiO_2 particles.
SiO_2(57)/MPFR(43)	Figs. 15 and 16	Transparent-red. Polydisperse oblate SiO_2 particles resting on MPFR matrix.
SiO_2(60)/MPFR(40)/HF	Figs. 17 and 18	Transparent-red. Quasi-elliptical SiO_2 particles can be seen on the surface and body of the substrate surrounded by polymer matrix.
SiO_2(63)/MPFR(37)/HF	Figs. 19 and 20	Transparent-red. Cubic SiO_2 crystals (Fig. 19) and coalesced SiO_2 (Fig. 20) particles on a smooth silica-resin medium.
SiO_2(64)/MPFR(36)		Transparent-red. Quasi-spherical SiO_2 particles are homogeneously distributed inside the MPFR matrix.
SiO_2(64)/MPFR(36)/HF	Figs. 21 and 22	Opaque-red. Flakes of coalesced SiO_2 particles. Crystallization of silica is apparent.

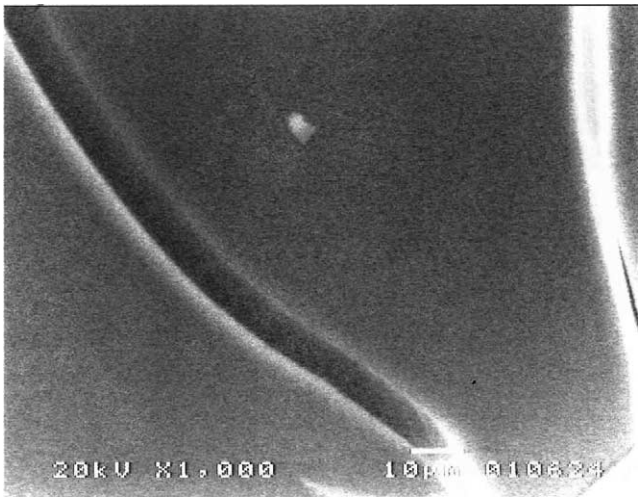

Fig. 5. SEM photograph of PFR(100).

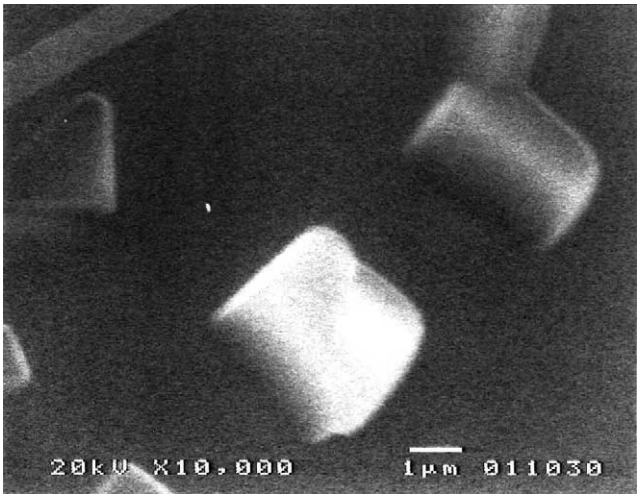

Fig. 7. Enlarged SEM view of crystals in sample SiO_2(55)/PFR(45)/HF.

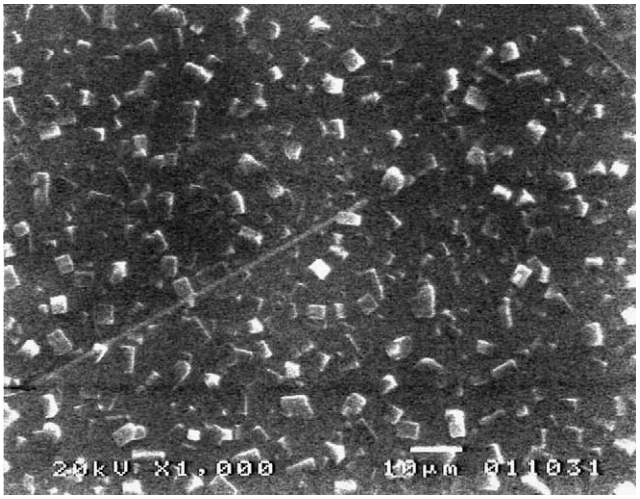

Fig. 6. SEM photograph of SiO_2(55)/PFR(45)/HF showing SiO_2 crystals.

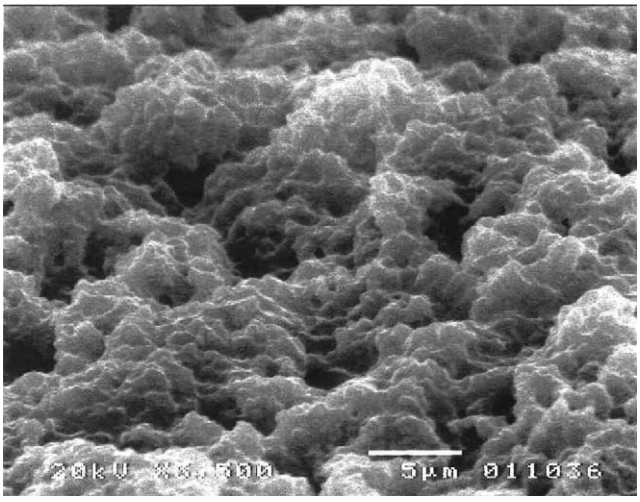

Fig. 8. SEM fracture surface of SiO_2(55)/PFR(45)/HF showing coalesced SiO_2 particles.

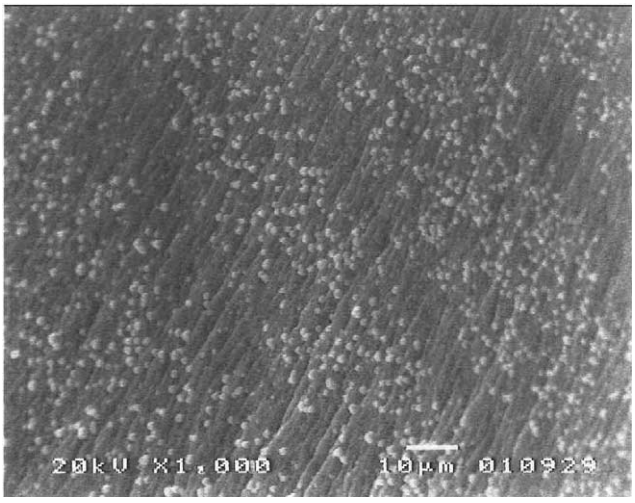

Fig. 9. SEM photograph of SiO_2(57)/PFR(43)/HF.

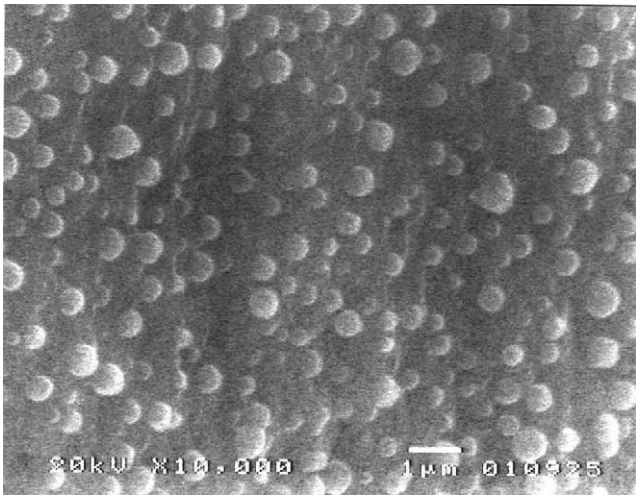

Fig. 10. Enlarged SEM photograph of SiO_2(57)/PFR(43)/HF.

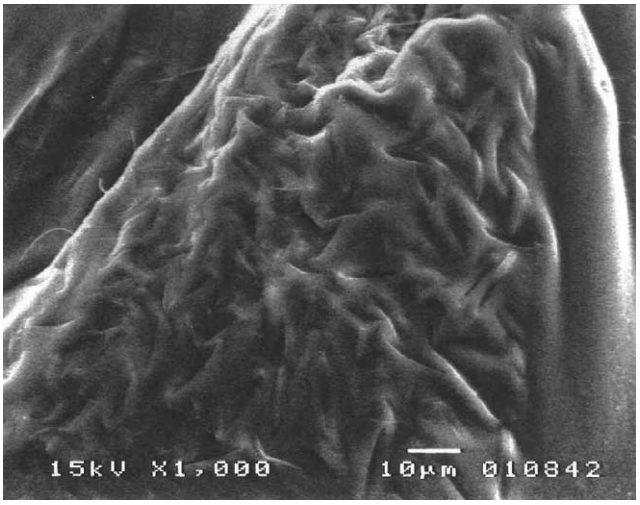

Fig. 11. SEM photograph of MPFR(100).

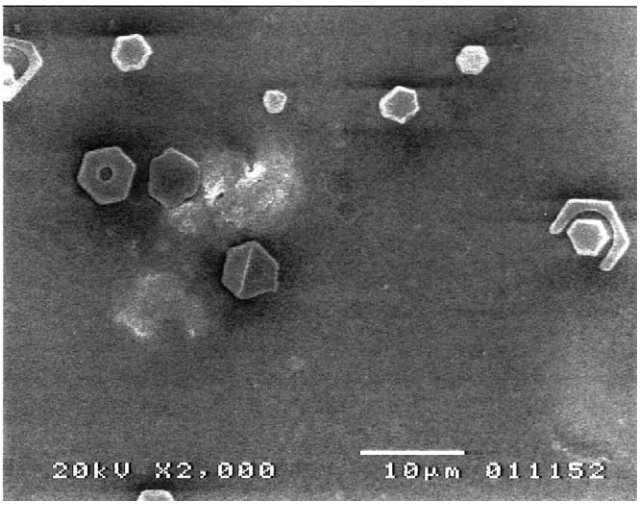

Fig. 12. Crystalline particles resting on the surface of SiO_2(40)/MPFR(60)/NH_3.

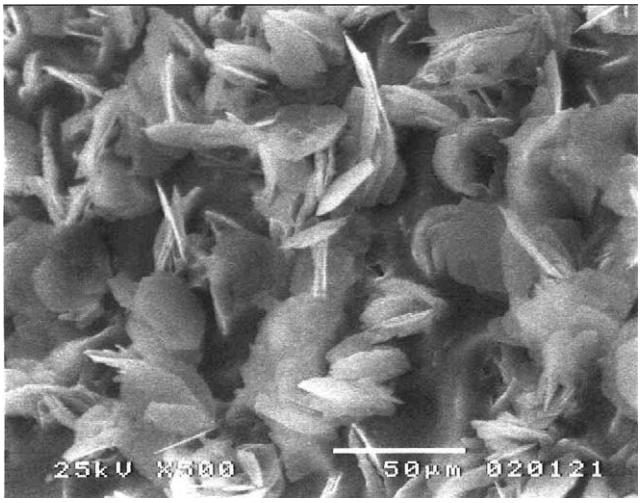

Fig. 13. Flake-like crystals in sample SiO_2(40)/MPFR(60)/NH_3.

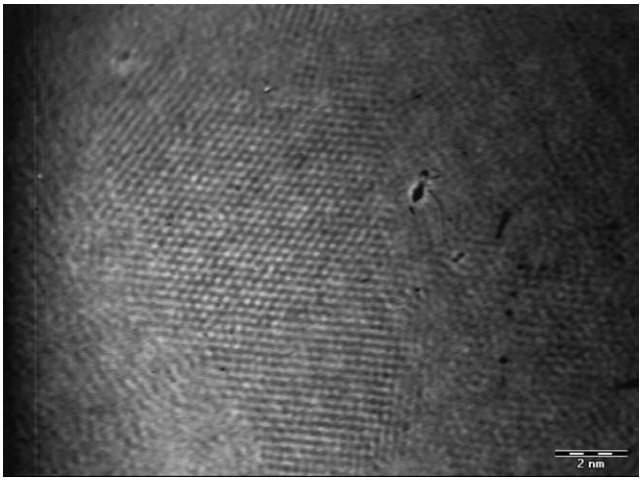

Fig. 14. High Resolution TEM micrograph of of SiO_2(40)/MPFR(60)/NH_3.

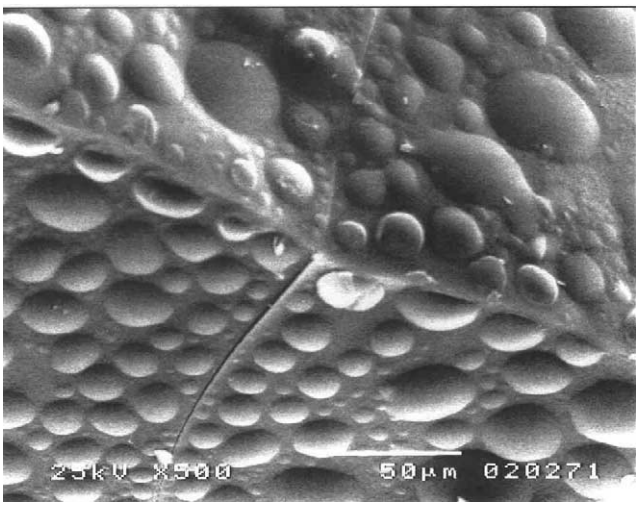

Fig. 15. Silica particles embedded in PFR resin in sample SiO_2(57)/MPFR(43).

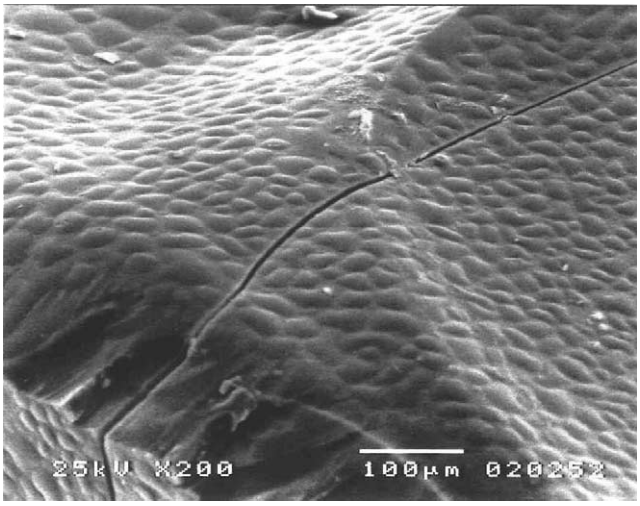

Fig. 16. SEM photograph of the surface of sample SiO_2(57)/MPFR(43).

translucent when some phase segregation arises between SiO_2 and MPFR matrix; the silica aggregates becoming significantly larger than those existing in transparent substrata.

SiO_2(57)/MPFR(43) (Figs. 15 and 16) and SiO_2(60)/MPFR(40)/HF (Figs. 17 and 18) hybrids are highly transparent specimens, in which the repartition of silica particles throughout the volume of these substrata seems to be homogeneous. The sizes of silica particles decrease from ≈ 30 µm in sample SiO_2(57)/MPFR(43) to ≈ 10 µm in sample SiO_2(57)/MPFR(43). In the case of SiO_2(57)/PFR(43), the silica particles are not embedded in the polymer matrix (see Figs. 9 and 10).

SiO_2(63)/MPFR(37)/HF sample brings about some interesting characteristics (see Figs. 19 and 20). It seems that in this solid, the concentration of SiO_2 is large enough to provoke the segregation of cubic silica

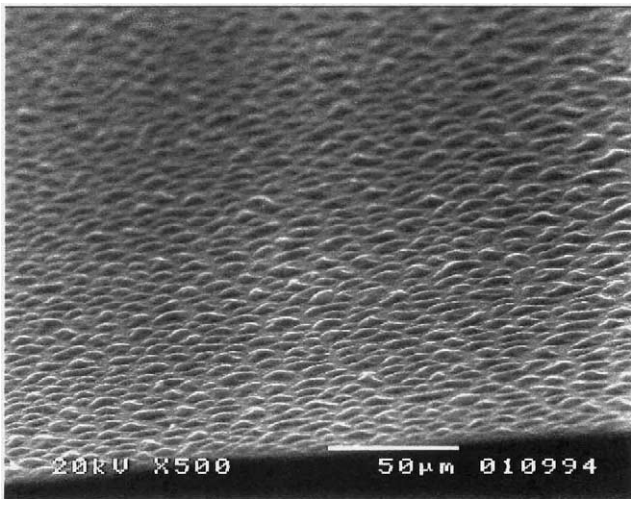

Fig. 17. SEM photograph of SiO_2(60)/MPFR(40)/HF.

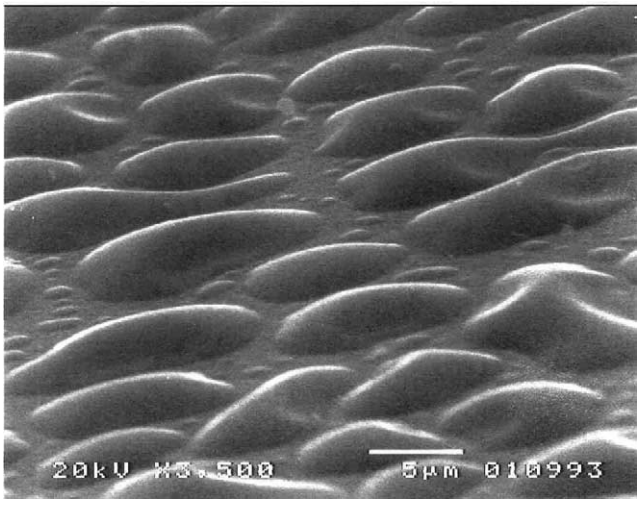

Fig. 18. Enlarged SEM view of the surface of SiO_2(60)/MPFR(40)/HF.

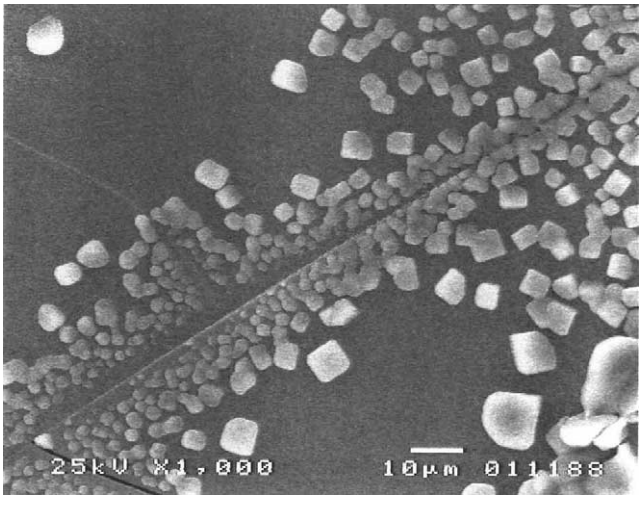

Fig. 19. Segregated crystals on the surface of sample SiO_2(63)/MPFR(37)/HF.

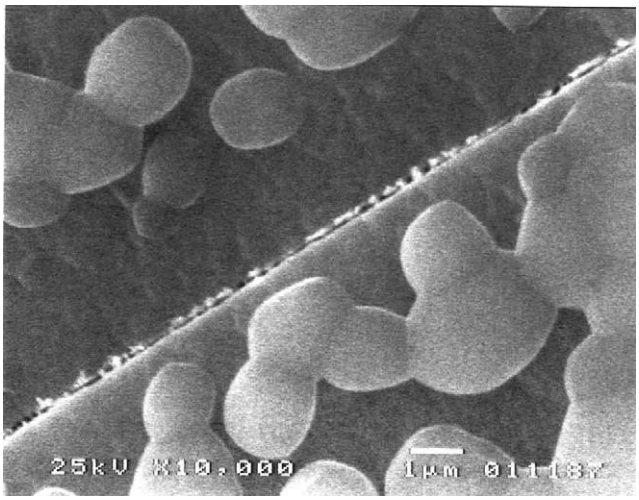

Fig. 20. Coalesced silica aggregates in sample SiO_2(63)/MPFR(37)/HF.

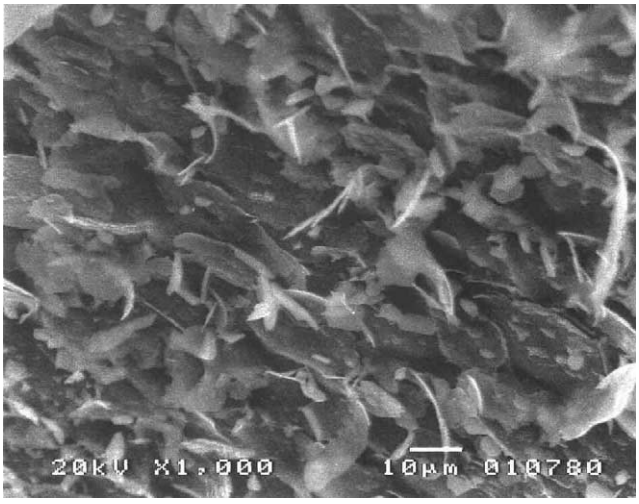

Fig. 21. Flake-like aggregates in sample SiO_2(64)/MPFR(36)/HF.

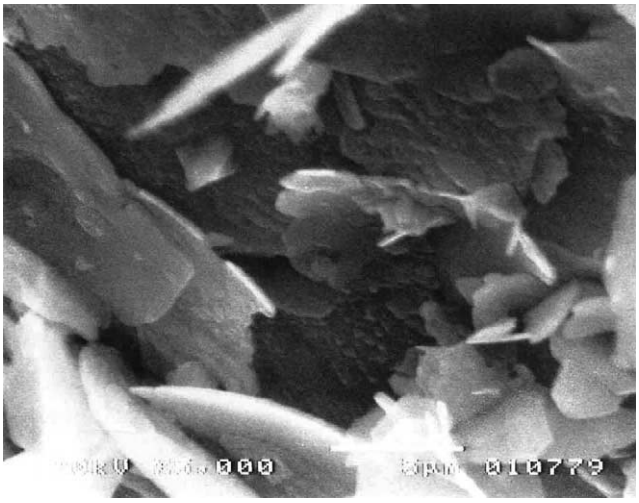

Fig. 22. Enlarged SEM view of flake-like aggregates in sample SiO_2(64)/MPFR(36)/HF.

crystals from the silica–MPFR matrix. The onset of phase separation between pure silica and hybrid matrix in these materials appears to be around 63% wt. SiO_2. The noticeable SiO_2 crystallization that occurs in this sample may be induced by: (i) an excess of OH groups on the surface of SiO_2 particles [19], or (ii) the action of the HF catalyst, since some of the samples showing SiO_2 crystals (i.e. SiO_2(55)/PFR(45/HF, SiO_2(63)/MPFR(37)/HF) were prepared in the presence of HF.

Sample SiO_2(64)/MPFR(36)/HF depicts a morphology that is classical of opaque materials (Figs. 21 and 22). Lamella of SiO_2 particle aggregates can be seen segregating from the MPFR polymer matrix.

4. Conclusions

Organic–inorganic hybrids can be successfully synthesized by the sol-gel processing of silica in the presence of a phenolic-aldehydic resin. This resin can be either used as prepared or can be chemically modified through the introduction of carboxylic end-groups. Hybrid materials resulting from the reaction of TEOS and functionalized MPFR resin display chemical bonds at the interface between silica particles and polymer matrix, thus suggesting that the interaction between these two components is due to a hydrogen bonding between silanol and phenolic carboxyl hydroxyl groups (or phenolic hydroxyl groups). Interactions between silica and phenolic resin groups affect the compatibility of phases in the system. Hence, the morphological, thermal and optical properties of these hybrid materials can be deeply influenced by the concentration of reactants and the nature of the phenolic-formaldehydic resin.

The opacity characteristics of these hybrid specimens are determined by an inhomogeneous repartition of polydisperse silica aggregates in the polymer resin matrix. On the other hand, transparency-translucency is favored by a more homogeneous repartition of silica particles throughout the polymer matrix as well as by a strong chemical interaction across the SiO_2–MPFR interface. The choice of gelation catalyst also influences the optical and thermal properties of silica-phenolic-formaldehydic polymer resin hybrids.

Morphological (SEM) and thermal (TGA) properties lead to regard this hybrid material as potentially relevant for future technological applications, since the microscale morphology and interfacial properties of these substrates provide hybrid materials of enhanced thermal and optical properties. The presence of the MPFR resin affects SiO_2 particle nucleation and growth, consequently influencing the final transparency and microphase dispersion characteristics of the hybrid material.

Further studies of these hybrid microstructures, which are related to other physical and chemical characteristics including a full mechanical characterization, are currently under way.

Acknowledgements

The authors gratefully acknowledge C. Peza, S. Espinoza, J. Cañetas, L. Rendón, A. Sánchez and R. Hernández for their helpful contributions to this work.

References

[1] A.J.E. Pope, in: Y.A. Attia (Ed.), Sol-Gel Processing and Applications, Plenum Press, New York, 1994, p. 119.
[2] B.M. Novak, Adv. Mater. 5 (1993) 422.
[3] L. Xiaochun, T. King, in: A.K. Cheethum, C.J. Brinker, M. Mecarthey, C. Sanchez (Eds.), Better Ceramics through Chemistry VI, vol. 346, Mat. Res. Soc. Symp. Proc, USA, 1994, pp. 541–546.
[4] J. Wen, G. Wilkes, Chem. Mater. 8 (1996) 1667.
[5] G. Wilkes, H.-H. Huang, R.H. Glaser, New inorganic-organic hybrids materials through the sol-gel approach, in: Silicon-Based Polymer Science: a Comprehensive Resource, Advances in Chemistry Ser. 224, American Chemical Society, Washington, DC, 1990, pp. 207–226.
[6] K. Haraguchi, Y. Usami, K. Yamamura, S. Matsumoto, Polymer 39 (1998) 6243.
[7] T. Komatsubara, Polymer Materials and Technology. Part I: Introduction to Thermosetting Resins, Osaka Municipal Technical Research Institute, JICA, Japan, 1993, p. 6.
[8] G. Hernández-Padrón, R.M. Lima, R. Nava, M. García-Garduño, V. Castaño, Adv. Polymer Technol. 21 (2002) 116.
[9] B.N. Colthup, H.L. Daly, E.S. Wiberley, Introduction to Infrared and Raman Spectroscopy (Chapters 5, 8 and 9), Academic Press, San Diego, CA, 1990.
[10] G. Orcel, J. Phalippou, L.L. Hench, J. Non-Cryst. Sol. 88 (1986) 114.
[11] J. Ferraro, M. Manhari, J. Appl. Phys. 43 (1972) 4595.
[12] B. Schrader, Infrared and Raman Spectroscopy: Methods and Applications (Chapter 3 and 4), VCH, Berlin, Germany, 1995.
[13] L.R. Pecksok, L.D. Shelds, Modern Methods of Chemical Analysis, Wiley and Sons, New York, 1990, pp. 209–216.
[14] M. Choi, I. Chung, J. Lee, Chem. Mater. 12 (2000) 2977.
[15] G. Hernández, R. Rodríguez, J. Non-Cryst. Sol. 246 (1999) 209.
[16] J.M. Lin, M.C.C. Ma, Y.F. Wang, D.H. Wu, C.S. Kuang, J. Polym. Sci.: Part B: Polym. Phys. 38 (2000) 1699.
[17] K. Haraguchi, Y. Usami, Chem. Lett. 1997 (1997) 51.
[18] K. Haraguchi, Y. Usami, Y. Ono, J. Mater. Sci. 33 (1998) 3337.
[19] T. Woignier, J. Phalippou, J. Mater. Sci. 25 (1990) 3118.